Apelin-mediated deamidation modification of HMGA1 promotes tumorigenesis by enhancing SRBEP1 activity and Lipid Synthesis

Li Zhang
Precision Medicine Research Center, West China Hospital of Sichuan University
Yihan Zhu
Laboratory of Pathology, Key Laboratory of Transplant Engineering and Immunology, NHC, West China Hospital, Sichuan University
Ying Yang
Precision Medicine Research Center, West China Hospital of Sichuan University
Hong Bu
Laboratory of Pathology, Key Laboratory of Transplant Engineering and Immunology
Hong Huang
Laboratory of Pathology, Key Laboratory of Transplant Engineering and Immunology
Jingjing Ran
Laboratory of Human Diseases and Immunotherapies, West China Hospital
Liwen Qin
Administration of Research Park, West China Hospital, Sichuan University
Yinyun Ni
Precision Medicine Research Center, West China Hospital of Sichuan University
Menglin Yao
Precision Medicine Research Center, West China Hospital of Sichuan University
Tingting Song
Precision Medicine Research Center, West China Hospital of Sichuan University
Mufeng Li
Department of Nuclear Medicine, West China Hospital, Sichuan University
Yongfeng Yang
Precision Medicine Research Center, West China Hospital of Sichuan University
Tingting Guo
Department of Hematology, West China Hospital, Sichuan University, China
Ningning Chao
Department of Hematology, West China Hospital, Sichuan University, China
Zhiqing Liu
Department of Hematology, West China Hospital, Sichuan University, China

Weiming Li (weimi003@scu.edu.cn)
Department of Respiratory and Critical Care Medicine, State Key Laboratory of Biotherapy, West China Hospital, Sichuan University, Chengdu, Sichuan

Article

Keywords: Apelin, HMGA1, SREBP1, lipid metabolism, deamidation modification, lung cancer cells

Posted Date: November 3rd, 2020

DOI: https://doi.org/10.21203/rs.3.rs-95255/v1

Abstract

Apelin is a ligand of the G protein-coupled receptor that promotes tumor growth in malignant cancers. However, the molecular mechanisms through which apelin promotes tumorigenesis are unknown. Here, we confirmed that apelin promotes tumorigenesis in lung cancer cells by increasing the synthesis of fatty acids, which induces abnormal lipid metabolism. Apelin interacts with high-mobility group A HMGA1 and mediates sterol-regulatory-element-binding protein 1 (SREBP1) activity, which is required for lung tumorigenesis and lipid metabolism. Deamidation modification of HMGA1 is regulated by apelin enhanced SRBEP1 activity and lipid synthesis. Moreover, deamidated HMGA1 can enhance the formation of the apelin-HMGA1-SREBP1 complexes and increases SREBP1 activity, which induces abnormal lipid metabolism. As an energy regulator, Apelin forms a multi-protein complexes with HMGA1 to increase of lung cancer cells viability. Our results indicate that apelin is important in lipid metabolism and cancer cell proliferation.

Introduction

Apelin is a member of adipokines and is abundantly secreted by adipocytes[1]. Apelin has several functions, including energy metabolism, fluid homeostasis and angiogenesis[2]. Apelin greatly increases the likelihood of malignant tumors, such as lung cancer[3], glioblastoma[4], ovarian cancer[5], colon cancer[6], and hepatocellular carcinoma[7] and is associated with a poor prognosis, which suggests apelin might promote tumorigenesis. Exogenous apelin has as anti-apoptotic effect and stimulates the proliferation of colon cancer cells through the JAG-1/Notch3 signalling pathway[8]. Apelin also increases the invasiveness of breast cancer[9], gastric cancer[10], and the colon cancer cells by a matrix metalloproteinase (MMP)-dependent manner[11]. In addition, apelin is an important proangiogenic factor and could be a potential target in tumor therapy by interfering with angiogenesis[12]. However, the molecular mechanisms of apelin in tumorigenesis are unknown.

Metabolic reprogramming, including both the Warburg effect (aerobic glycolysis) and abnormal lipid synthesis, is one of the hallmarks of cancer, which maintains cell proliferation in a severe microenvironment and provides energy to support the metastasis of cancer cells[13,14]. Increased glucose consumption is a major source of energy in tumor cells, not only for glycolysis, but for increased lipogenesis[15]. Activated de novo lipogenesis accelerates tumor cell growth, participates in immune evasion, and is closely associated with poor prognosis in many tumors[16].

The important molecules in lipogenesis include acetyl-CoA carboxylase (ACC) 1, which catalyzes the ATP-dependent carboxylation of acetyl-CoA to form malonyl-CoA[17]. The multi-domain enzyme fatty acid synthase (FASN) uses malonyl-CoA and acetyl-CoA to catalyze subsequent successive reactions to form fatty acids[18].

Sterol regulatory-element-binding protein 1 (SREBP1), a member of the transcription factor family, is also important in fatty acid synthesis. As an inactive precursor, SREBP1 is found in the endoplasmic reticulum and in the proteolytic release of an N-terminal fragment in Golgi-activated SREBP1 and promotes the expression of lipogenic genes[19,20]. Apelin might also regulate glucose metabolism by restoring glucose tolerance and increasing glucose metabolism in insulin-resistant mice[21]. However, apelin inhibits lipid accumulation in human hepatoma cells (Hep3B) and in primary mouse hepatocytes. It also suppresses the expression of sterol regulatory element-binding protein 1c (SREBP-1c) and glycerol-3-phosphate acyltransferase (GPAT)[22]. But, whether apelin promotes the proliferation and metastasis of tumors by regulating abnormal lipogenesis is unknown.

In addition to glucose, glutamine is also a source of carbon for replenishing the tricarboxylic acid (TCA) cycle and produces the precursor (glutathione) to nucleotides and lipid synthesis by reductive carboxylation[23]. The glutamine amidotransferases (GATs) are a family of metabolic enzymes that extract nitrogen from glutamine to synthesize nucleotides, amino acids, glycoproteins, and the enzyme cofactor, nicotinamide adenine dinucleotide (NAD), which are required for cell growth and proliferation[24]. Deamidation modification increases the affinity of protein interactions and promotes cell metabolism for cancer-cell proliferation and tumorigenesis. For example, deamidating the RelA subunit of NF-kB in cancer cells promotes aerobic glycolysis and increases tumorigenesis. This post-translational modification switches RelA function from increasing the expression of NF-kB-responsive genes to increasing the production of glycolytic enzymes, thus shunting the cell's inflammatory response to aerobic glycolysis[25]. Whether apelin is involved with deamidation modification in promoting tumorigenesis is unknown.

In this study, we created lung cancer cells lines to establish apelin-overexpression (A549 and H1975) and knock-down (H460) cells to investigate the mechanism of apelin in regulating lung cancer. We found that apelin promoted proliferation of lung cancer cells by increasing fatty acid de novo synthesis. We identified a new mechanism in which apelin formed complexes with HMGA1 and SRBEP1, deamidates HMGA1, and elevates SRBEP1 activity, which results in abnormal lipid metabolism.

Results

Apelin Expression was Increased in Lung Cancer Tissues

In this study, the expression of apelin in tissue samples of patients with lung cancer was detected by immunohistochemistry. Of the 51 patients enrolled in the study (32 men and 19 women), 24 had adenocarcinoma of the lung tissues (LUAD) and 27 had squamous carcinoma of the lung tissues (LUSC; Supplementary Table 1). In addition to 51 resected tumor samples, 39 distant healthy tissues were used as controls. Staining intensity was classified as low or high (Fig. 1a). Apelin expression was significantly higher in tumor tissues than in normal tissues (Fig. 1a). Kaplan-Meier analysis indicated that increased apelin expression was related to poorer survival of lung cancer patients, although not significantly so

(P=0.362; Fig. 1b). As in our previous study, Apelin expression was markedly elevated in lung tumor tissues.

Apelin Increased the proliferation of Lung Cancer Cells

To further explore the functions of apelin in lung cancer, we first analyzed the expression of apelin in cell lines from both tumor (A549, H1299, H446, H1975, and H460) and normal lung tissue (HBE). The expression of apelin was higher in H1299 and H460 cells in both mRNA and protein concentrations (Fig. 1d and Supplementary Fig. 1a) than in A549, H1975, and H446 (Fig. 1d).

In the next study, A549 (A549-OE) and H1975 (H1975-OE) were selected for apelin stable overexpression (Fig. 1e), and H460 (H460-KD) (KD, knock-down) was used for sh-RNA knockdown of apelin and restored with Apelin(KE) (Supplementary Fig. 1b). Overexpression of apelin increased cell viability (Fig. 1f) and colony formation (Fig. 1g and Supplementary Fig. 1c) in A549 and H1975 cells. Decreased G1 phase (A549) and enhanced S phage (A549 and H1975) were also observed in the A549-OE and H1975-OE groups (Fig. 1h). Knock down of apelin greatly suppressed cell viability and colony formation, whereas re-expression of apelin rescued the cellular proliferation in H460-KD cells (Supplementary Fig. 1d,e).

In addition, we found that knock-down expression of apelin in A549-OE substantially reduced cell viability and colony formation after apelin-siRNA treatment (Supplementary Fig. 1f-h). These results confirmed that apelin enhances cellular proliferation and colony formation in lung cancer cells. Finally, A549-OE and –NC cells implanted into nude mice resulted in subcutaneous tumor formation and increased tumor formations (Fig. 1i). Tumor volume (Fig. 1j), and tumor weight (Supplementary Fig. 1i) in A549-NC and -OE group were detected from 6 weeks after implantation. All these results indicate that apelin promoted tumor growth in lung cancer cells.

Apelin Induced Metabolic Reprogramming in Lung Cancer Cells by Enhancing Lipid Metabolism

To investigate how apelin promotes tumor formation, A549-OE and –NC cells detected by RNA-Seq revealed enrich variation were metabolic-related genes in A549-OE cells (Fig. 2a), indicating changes in apelin expression are associated with changes in metabolism. Quantitative PCR showed that fatty acid synthesis-related genes were upregulated in both A549-OE (OE, over-expression) and H1975-OE cells, including GLUT4, FASN, ACC1, and SREBF1(Fig. 2b), which were also observed in protein concentrations (Fig. 2c).

Glucose was the most important material in both the tricarboxylic acid cycle (TCA) and lipid synthesis (Fig. 2d). To test whether apelin uses glucose as an energy source to increase fatty acids synthesis, both A549-OE and –NC (NC, negative controls) cells were labelled with [U-^{13}C6] glucose to measure carbon incorporation into newly synthesized fatty acids over 24 hours. The results indicated that apelin promoted the synthesis of both saturated fatty acids (palmitate, stearate, and myristate; Fig. 2e) and unsaturated fatty acids (palmitoleate, oleate, and arachidonate (Supplementary Fig. 2a). The intermediaries of the TCA cycle were mostly decreased in A549-OE cells except citrate (Fig. 2f). Glucose

uptake was also elevated in A549-OE and H1975-OE cells (Fig. 2g), and apelin-siRNAs reduced the elevated glucose uptake (Supplementary Fig. 2b), which indicated that apelin preferentially used glucose as source for lipogenesis.

We next used nile red staining to detect the lipid concentration on apelin-overexpression or knock-down cells. Lipid components markedly were greatly increased in A549-OE and H1975-OE cells (Fig. 2h and Supplementary Fig. 2c). Instead, glucose uptake declined, and lipid components accumulation was restrained in H460-KD cells (Fig. 2i and Supplementary Fig. 2d).

To verify the effect of lipids on cell proliferation, H460-negative control (control, H460) and apelin knock-down cells (KD, H460) cells were grown in palmitate and then plated into media containing either regular fetal bovine serum (FBS) or delipidated FBS (FCS) in the presence or absence of exogenous palmitate. Cellular growth in apelin knock-down cells (KD, H460) was markedly lower than in controls(control, H460) in medium containing regular FBS, a result that was even more pronounced in delipidated FBS, but apelin-KD cells (KD, H460) were rescued by exogenous palmitate (Fig. 2j).

Finally, nile red staining in H460-control and –KD cells, as well as those treated and untreated with palmitic acid in a medium containing FBS or FCS, also confirmed that apelin knock-down greatly decreased lipid content (Fig. 2k). Taken together, these results indicate that apelin can induce metabolic reprograming by promoting lipid synthesis.

SREBP1 was Important in Apelin-Mediated Lipid Metabolism

Our study indicated that apelin markedly promoted the expression of sterol-regulatory-element-binding proteins 1 (SREBP1; Fig. 2b), a transcription factor that induces the expression of genes synthesizing cholesterol and fatty acids[26]. High glucose stimulation enhances SREBP1 expression and prevents SREBP1 binding to ER-anchored, insulin-induced gene protein (Insig1) and activates the expression genes involved in lipid metabolism[14]. Therefore, we further investigated whether SREBP1 was involved in apelin-induced abnormal lipid metabolism.

Overexpression of apelin promoted mature (SREBP1-N) and precursor-SREBP1 (SREBP1-P) expression in A549-OE and H1975-OE cells (Fig. 3b). Cellular immunofluorescence experiments confirmed that apelin promoted the expression of endogenous SREBP1 and the localization of SREBP1 to the Golgi apparatus and to the nucleus in A549-OE cells (Fig. 3b), a finding further confirmed by nuclear protein detection (Fig. 3c). To further confirm the effect of apelin on SREBP1, knock-down apelin in H460 cell(H460-KD), SREBP1 expression level and activity were reduced, but were rescued with reconstituted of apelin in H460-KE cell (Fig. 3d).

Next, SREBP1-siRNA was introduced to confirm the function of SREBP1 in apelin-mediated lipid metabolism. We found that inhibiting SREBP1 decreased both mature and precursor-SREBP1, as well as the lipid synthesis-related molecules, ACC1 and FASN, in both protein (Fig. 3e) and mRNA concentrations (Fig. 3f). Nile red staining revealed that lipid synthesis was also inhibited in A549-OE and H1975-OE cells

in the knockdown of SREBP1 (Fig. 3g). Finally, si-SREBP1 also inhibited cell viability in A549-OE and H1975-OE cells (Fig. 3h). These results strongly suggest the importance of SREBP1 in abnormal lipogenesis and cell viability mediated by apelin.

Apelin Improved SREBP1 Activity by Forming Apelin-SREBP1 Complexes and Inhibiting SREBP1-Insig1 Binding

Th above results confirmed that apelin promotes SREBP1 activity, but the molecular mechanism is still unknown. Insulin-induced gene protein 1 (Insig1) could bind to SREBP1 on the endoplasmic reticulum, restrain the movement of SREBP1 to the Golgi apparatus, inhibit the N-terminal cleavage of SREBP1 into the nucleus, and regulate the expression of lipid metabolism genes. Therefore, a co-immunoprecipitation (Co-IP) assay was performed to verify whether apelin regulated the binding of SREBP1 and Insig1. Overexpression of apelin markedly inhibited SREBP1 from combining with Insig1 in A549-OE and H1975-OE cells (Fig. 4a,4b). To the contrary, knockdown of apelin greatly increased the binding of SREBP1 to Insig1, and re-expression of apelin in H460-KD cells re-inhibited SREBP1-Insig1 binding (Fig. 4c).

Next, we investigated whether apelin inhibited SREBP1 from binding to Insig1 by direct interaction with SREBP1. Using apelin as a bait protein, the Co-IP result confirmed that binding of apelin to SREBP1 was increased in A549-OE and H1975-OE cells (Fig. 4d,e). Our results indicated that apelin promoted SREBP1 activity by dissociating SREBP1 with Insig1 to forming an apelin-SREBP1 complexes.

Apelin-HMGA1 Complexes Facilitates Lipid Metabolism and Lung Cancer Cell Proliferation

Several molecules contribute to metabolic reprograming in malignant tumors. High Mobility Group A1 (HMGA1) is an architectural transcription factor involved in regulating lipid metabolism by promoting GLUT3 expression[27]. Cancer Genome Atlas (TCGA) data analysis showed that expression of HMGA1 was substantially increased in tissues of patients with lung adenocarcinoma (LUAD) and squamous carcinoma (LUSC; Supplementary Fig. 3a,b). Furthermore, elevated HMGA1 concentrations were associated with poor prognosis in patients with LUAD (P=0.0027; Supplementary Fig. 3c) but not with survival in patients with LUSC (data not shown). In addition, Pearson correlation analysis revealed that HMGA1 concentration was related to multiple lipid synthesis-related genes (Supplementary Fig. 3d), which suggested the importance of HMGA1 in lipid metabolism. Therefore, we speculated that HMGA1 might be involved in apelin-mediated abnormal lipid synthesis.

We first observed that the expression of HMGA1 was increased in A549-OE and H1975-OE cells (Supplementary Fig. 3e and Fig. 5a) and decreased in H460-KO cells (Supplementary Fig. 3f,g). A Co-IP assay revealed increased binding of apelin to HMGA1 in A549-OE and H1975-OE cells (Fig. 5a). In addition, apelin and HMGA1 were co-localized in the nucleus of A549 -OE cells (Fig. 5b).

When HMGA1-siRNA was introduced to confirm this observation, we found that knockdown HMGA1 greatly inhibited cell viability (Fig. 5c) and colony formation in A549-OE and H1975-OE cells (Fig. 5d). Moreover, glucose uptake capacity and acetyl-CoA activity were also restrained in A549-OE and H1975-OE

cell after si-HMGA1 treatment (Fig. 5e,f), as with the expression of lipid synthesis genes, including ACC1, SREBP1, and FASN (Fig. 5g).

The most interesting observation was that si-HMGA1 inhibited SREBP1 concentrations in both the mature (SREBP1-N) and precursor (SREBP1-P) forms in A549 -OE and H1975-OE cells (Fig. 5h), which suggested a close relationship between HMGA1 and SREBP1 in abnormal lipid metabolism induced by apelin. Finally, cholesterol - modified si-HMGA1 in the treatment of subcutaneous tumors in nude mice indicated that si-HMGA1 slightly reduced the tumor volume and weight of A549-OE engrafted mice (Fig. 5i,j). Oil red staining confirmed that lipid components also decreased more in si-HMGA1 tumor tissues than in A549-OE tissues (Fig. 5k). These results confirm that HMGA1 is important in apelin-mediated abnormal lipid metabolism in lung cancer cells.

Deamidated HMGA1 Increased the Binding of Apelin to HMGA1 and Increased the Activity of SREBP1

Our study confirmed that HMGA1 can increase abnormal lipid synthesis by forming an HMGA1-apelin complexes (Fig. 5a); however, the binding regions in HMGA1 and the regulation mechanism are unknown. Immunoprecipitation and mass spectrometry revealed that two fragments of the HMGA1 protein directly bind to apelin. We constructed three deficient mutant plasmids of HMGA1: delete 1 and delete 2 were deficient in the binding region of 30-47 and 92-107 respectively, and delete 3 was co-deficient in two binding fragments (Fig. 6a). The three described above deficient mutant plasmids of HMGA1(HMGA1-Del1, Del2, Del3), as well as HMGA1 full length control (HMGA1-FL/WT), were co-transfected into 293T cells. The results indicated that apelin interacted with wild-type HMGA1 (Fig. 6a and Supplementary Fig. 4a), but this interaction was sharply reduced in HMGA1 deletes 1 and 3, but not in delete 2 (Fig. 6a), which indicated that fragment 30-47 was the region important in binding HMGA1 to apelin.

In this region, Glu 32 was an important site that had undergone deamidation of glutamine into glutamate (Fig. 6a). In addition, expressions of many glutamine amidotransferases increased in A549-OE and H1975-OE cells (Supplementary Fig. 4b,c), which suggested that apelin might increase the expression of glutamine amidotransferases, induce deamidation in HMGA1, and increase the binding of apelin to HMGA1.

To confirm this hypothesis, glutamine amidotransferase inhibitor (DON) was used to investigate whether deamidation modification regulated the binding of HMGA1 to apelin. We found that DON reduced binding of apelin to HMGA1 (Fig. 6c). To confirm the importance of deamidation modification in apelin-HMGA1 interaction, two HMGA1 mutants, Q32E (glutamic acid, Glu) and Q32A (alanine, Ala), at a deamidation site resistant to deamidated were generated. Substituting Gln-32 with Glu, not Ala, increased binding of apelin to HMGA1 in both 293T (Fig. 6d) and A549-OE cells (Fig. 6e), showing that HMGA1 deamidation increased apelin-HMGA1 binding. Furthermore, we also found that HMGA1-WT and Q32E increased the viability of A549-OE cells compared with Q32A (Fig. 6f), as well as promoted mRNA expression of lipid metabolism genes (Fig. 6g). SREBP1 activity also was elevated in A549-OE and 293T cells with transfected HMGA1-WT and Q32E (Fig. 6h).

When we studied the effect of endogenous deamidation modification in lung cancer cells, we found that DON inhibited glutamine amidotransferases expression (Fig. 6i, Supplementary Fig. 4d) in A549-OE and H1975-OE cells and restrained apelin-HMGA1 interactions (Fig. 6j). DON treatment also reduced the expression of lipid-related genes in A549-OE and H1975-OE cells (Fig. 6k and Supplementary Fig. 4e,f). Finally, adding DON markedly restrained the viability of A549-OE cells (Fig. 6l). All these results indicated that deamidation modification of HMGA1 increased the binding affinity of apelin and HMGA1, subsequently activated SRBEP1, and promoted SREBP1-responsive lipogenesis.

Deamidated HMGA1 Promoted the Formation of Apelin-SREBP1-HMGA1 Complexes

We found that apelin can bind to SREBP1 and HMGA1 separately and that HMGA1 deamidation modification promoted the formation of an apelin-HMGA1 complexes and improved SREBP1 activity. However, whether HMGA1 directly interacts with SRBEP1 is unknown. Immunoprecipitation revealed that HMGA1 could interact with SREBP1 in A549-OE (Fig. 7a) and H1975-OE cells (Supplementary Fig. 5a), which indicated the formation of an apelin-SREBP1-HMGA1 complexes. Deamidated HMGA1 increased the activity of SREBP1, but whether it affected the binding of HMGA1 to SREBP1 was still unclear.

We found that si-HMGA1 and DON treatment increased the binding of SREBP1 to Insig1(Fig. 7b). Furthermore, si-HMGA1 and DON treatment both inhibited the formation of an apelin-SREBP1-HMGA1 complexes, then suppressed SREBP1 activity and the expression of lipogenic-related molecules (Fig. 7c,d). It illustrated that HMGA1 was essential for formation of multi-proteins complexes.

To further explore the relationship between apelin, HMGA1, and SREBP1, the 293T co-transfection experiment confirmed that apelin and HMGA1 both directly interact with SREBP1, while apelin can enhance the combination with HMGA1 and SREBP1(Fig. 7e). It was showed that apelin was key regulator to form of multiprotein complexes. To further confirmed whether deamidation modification promoted the formation of an apelin-HMGA1 -SREBP1complexes, it was showed multiprotein complexes was restrained in the presence of DON (Fig. 7f), like effect on A549-OE cell (Fig. 7c). The HMGA1-Q32E mutation increased the binding of SREBP1 to HMGA1(Fig.7g and Supplementary Fig. 5b) and dissociated SREBP1 from Insig1 in the presence or absence of apelin, whereas HMGA1-Q32A had no similar effect (Supplementary Fig. 5c,d), indicating that deamidation modification of HMGA1 competitively combined with SREBP1 and reduced the binding of Insig1 with SREBP1. We further confirmed that the HMGA1-Q32E mutation promoted the formation of an apelin-HMGA1-SREBP1 complexes both in lung cancer A549-NC and -OE cells, whereas Q32A had no effect (Fig. 7h). This phenomenon further illustrated that deamidated HMGA1 was essential for regulating the activity of SREBP1 and the interaction SREBP1 with Insig1. Deamidated HMGA1 acted independently to regulate the SREBP1 activity. Deamidation modification of HMGA1 also reduced Insig1-SREBP1 interaction in A549 cell (Supplementary Fig. 5e). Taken together, deamidation modification strongly enhanced the formation of an apelin-SREBP1-HMGA1 complexes and increased of SREBP1 activity.

Discussion

Development and progression of cancer are frequently associated with increased de novo lipogenesis in tumor cells. In this study, we confirmed that apelin had greatly increased concentrations in tissues from lung cancer tumors and promoted tumor growth in lung cancer cell lines. We then determined that apelin promoted lung cancer proliferation by enhancing lipid synthesis. We also identified two important lipid-regulating factors, HMGA1 and SREBP1, that, when combined with apelin, formed an apelin-HMGA1-SREBP1 complexes that increased lipid metabolism in lung cancer cells. We identified a new mechanism through which apelin promoted tumorigenesis. The theoretical model (Fig.8) illustrated that overexpressed apelin in lung cancer cells resulted in increasing of glucose uptake and weakened oxidative phosphorylation for enhancing lipogenesis. This occured, at least partially, due to apelin-mediated deamidation modification of HMGA1. Apelin interacted with HMGA1 and regulated the deamidation modification of HMGA1. Deamidation of HMGA1 increased the binding of HMGA1 to apelin, subsequently bound to SREBP1 and inhibited the interaction SREBP1 with Insig1 on endoplasmic reticulum (ER). SREBP1 complexes dissociated from Insig1, transported to the Golgi where SREBP1 released the transcriptionally active N-terminal fragment and entered the nucleus with HMGA1 and apelin to promote the expression of lipid synthesis genes.

Although apelin had been reported to enhance proliferation of multiple tumor cells, the mechanism was still unknown. Apelin is secreted by adipocytes and affects several biological functions by regulating glucose metabolism and fatty acid oxidation[28,29]. Apelin stimulates glucose uptake by regulating AMP-activated protein kinase-(AMPK), MAPK/Erk-, and PI3K-Akt-dependent signaling pathways in normal tissues[21,30]. Here, we established that apelin induced abnormal lipogenesis by increasing the synthesis of both saturated (palmitate and stearate) and unsaturated fatty acids, as well as by up-regulating lipid-related genes, such as GLUT4, FASN, ACC1, and SREBP1.

High-mobility-group A (HMGA1) protein is a nonhistone chromatin remodeling protein and is a transcription enhancer in elevating oncogene expression by interacting with DNA and protein in cancer cells[31]. The HMGA1 protein regulates, and is critically important to, tumor progression in diverse malignancies[32]. HMGA1 increases glucose uptake and ATP production by stimulating the transcription of the glucose transporter GLUT3 by binding GLUT3 promoter in colon cancer[25]. Sterol-regulatory element binding protein 1 (SREBP1) is an important transcription factor in lipid synthesis that stimulates the expression of lipogenic genes[33]. Inactive SREBP1 binds to insulin-induced gene (Insig1) and is located in endoplasmic reticulum, whereas activated SREBP1 translocate to the nucleus and increase lipid synthesis in malignant tumor cells[34,35]. The results of the current study demonstrated that apelin interacted with HMGA1, reduced binding of SREBP1 to Insig1, and promoted SREBP1 trafficking from the endoplasmic reticulum to the Golgi for activating SREBP1.

Our study revealed that apelin induced deamidation modification of HMGA1 and increased the binding of apelin to HMGA1, which activated SREBP1 and induced the translocation of SREBP1, leading to increasing lipogenesis.

Glutamine amidotransferases (GATs), an enzyme important in regulating deamidation modification, extracts nitrogen for sustaining cell growth and proliferation[36]. Tumor-associated deamidation promotes the proliferation of cancer cells by inducing metabolic reprogramming[22]. We found that deaminated HMGA1 acted as a new substrate of apelin in enhancing lipogenesis. The SREBP1 activity can be regulated by deamidated HMGA1 independently. Deamidated HMGA1 was sufficient for SREBP1 trafficking and activation, and si-HMGA1 and glutamine amidotransferase inhibitor (DON) both restrained SREBP1-responsive lipid gene expression.

We also determined that HMGA1 Glu 32 was the most important deamidated-related region of HMGA1. The glutamate mutant of HMGA1-Q32D can enhance the binding to apelin and SREBP1 than wild-type HMGA1 and HMGA1-Q32A, increasing the expression of the lipid genes, including GLUT4, ACC1, and FASN, but the alanine mutant of HMGA1-Q32A had the opposite effect.

In conclusion, we identified an important mechanism of apelin in promoting the lung cancer cells proliferation. We also found that apelin, as well as the apelin-HMGA1-SREBP1 complexes, might be new candidate metabolic target for lung cancer therapy.

Materials And Methods

Reagents and Antibodies

Rabbit monoclonal HMGA1 antibody (1:2000, Cat. 7777); rabbit monoclonal SCD1 antibody (1:2000, Cat. 2794); rabbit monoclonal ACLY antibody (1:2000, Cat.13390); rabbit monoclonal ACC antibody (1:2000, Cat. 3676) were purchased from Cell Signaling Technology (Beverly, MA). Mouse monoclonal Apln antibody (1:1000, Cat. sc-2934/1); mouse monoclonal SREBP1 antibody (1:2000, Cat. sc-365513); mouse monoclonal FASN antibody (1:3000, Cat. sc-48357); mouse monoclonal GLUT4 antibody (1:1000, Cat. sc-53566); mouse monoclonal Insig1 antibody (1:2000, Cat. sc-390504) were from Santa Cruz Biotechnology (Santa Cruz, CA). Mouse monoclonal His Tag antibody (1:1000, Cat. ab213204) was purchased from Abcam (Cambridge, MA). Mouse monoclonal β-Actin antibody (1:3000, Cat. 60008-1-Ig); rabbit polyclonal Lamin B1 antibody (1:1000, Cat. 12987-1-AP); mouse monoclonal GAPDH antibody (1:2000, Cat. 60004-1-Ig); rabbit polyclonal Giantin antibody (1:1000, Cat. 22270-1-AP); rabbit polyclonal PKM2 antibody (1:2000, Cat. 15822-1-AP); rabbit polyclonal GFP Tag antibody (1:3000, Cat. 50430-2-AP); rabbit polyclonal Flag Tag antibody (1:3000, Cat. 20543-1-AP) were from Proteintech (Wuhan, China). Rabbit Polyclonal HA Tag antibody (1:1000, Cat. A190-106A) was from Bethyl Laboratories (Montgomery, TX). Hoechst (cat. 94403) was from Sigma-Aldrich (St. Louis, MO). Protein A/G beads were obtained from Beyotime (Shanghai, China). L-6-Diazo-5-oxonorleucine (DON) was from MCE (Shanghai, China).

Cell Culture and Transfection

H1975, A549, H446, H460, H1299 were purchased from Cell Bank of the Type Culture Collection Committee, Chinese Academy of Sciences (Shanghai, China). HBE and HEK293T were gifts from the transthoracic surgery department of West China Hospital of Sichuan University. HBE and HEK293T were

maintained in Dulbecco's modified Eagle's medium (DMEM, HyClone) supplemented with 10% fetal bovine serum (FBS, HyClone). H1975, A549, and other lung cancer cells were cultured in RPMI 1640. All cell cultures were supplemented with 1% penicillin/streptomycin, and cells were incubated at 5% CO_2 at 37 ºC. Plasmids were transfected with a lip3000 Transfection reagent (Thermo Fisher) following the manufacturer's instructions.

Lentivirus-Mediated Stable Cell Line Construction

To establish an apelin-knockdown cell line, H460 cells were transfected with the apelin shRNA Lentiviral Particles (Santa Cruz). Controls were also transfected with shRNA Lentiviral Particles (Santa Cruz). Apelin was restored by infecting apelin-knock down H460 cell with lentivirus expressing full-length human apelin cDNA (Santa Cruz). H1975 and A549 were infected with puromycin-resistant lentiviral apelin particles. Stable integrants were selected and maintained with puromycin (2 μg/ml).

Plasmid Construction and RNAi Transfection

All plasmids were constructed by Gene Inc. Both siRNAs targeting apelin (sc-44741) and HMGA1(sc-37115) were purchased from Santa Cruz. Transfection assays for plasmids or si-RNA were performed using Lipofectamine 3000 (Life Technologies) according to the manufacturer's protocol.

Cell Viability and Colony-Formation Assays

Cell viability was assessed with a CCK8 kit in 96-well culture plates, according to the manufacturer's instructions. For delipidated media, cells were first seeded in media containing regular 10% FBS, and the following day were switched into media containing 20% delipidated FBS (Gemini, Cat. 900-123) on treatment. Palmitate (Sigma Aldrich, Cat. P5585) rescue experiments were performed in delipidated FBS by cotreating cells, in 96-well plates, with palmitate conjugated to BSA. For colony-formation assays, cells were seeded at 800 per/well in 6-well culture plates. After 14 days, cells were fixed with ice methanol for 30 min and washed with PBS three times, combined with crystal violet staining solution buffer, and incubated for another 30 min. Finally, the cells were rinsed with PBS, air dried, and photographed.

RNA Isolation and Real-Time PCR Analysis

Cells were lysed in TRIzol Reagent (Life Technologies) to extract total RNA according to the manufacturer's instructions. Total RNA was then reverse-transcribed to cDNA using the iScript cDNA Synthesis kit (Bio-Rad). The resulting cDNA underwent quantitative PCR with gene-specific primers in the presence of SYBR Green PCR master mix (Bio-Rad) using a Step-One-Plus Real-Time PCR System (Bio-Rad). Some metabolism-relative genes primers were cited from reference[14]. All primers are listed in Table S2.

Immunohistochemistry Staining and Immunofluorescence

The Department of Pathology, West China Hospital, Sichuan University, provided specimens of primary lung tumor tissues and normal pulmonary tissues surgically resected from patients treated without radiotherapy and chemotherapy. Paraffin embedding, tissue sectioning (5-μm) for tissues and immunohistochemical staining were performed as previously described[3]. Staining intensity was classified as low or high. Then, 8-mm-thick, fresh frozen tissues were mounted on glass slides for lipid Oil Red O staining to assess tumor lipid contents according to the manufacturer's instructions (Baso Diagnostics).

For nile red staining, cells were added to 100 ul of Hoechst (0.5 mmol/l) and stained for 10 min in a 96-well plates, then nile red buffer was added for 10 min. Cells were washed with PBS for 10 min and their fluorescence intensity was measured (Bio-Tek). To measure immuofluorescence, cells (20×10^4) were placed on glass coverslips in media containing 24-well plates. After transfection, cells were fixed with ice-methanol for 30 min and then blocked with fetal calf serum for 1 hr. A secondary antibody was added and the cells were incubated for 1 hr after adding a primary antibody. Finally, cells were counterstained with DAPI.

Nuclear and Cytoplasmic Extraction

Nuclear and cytosolic extraction was performed using the NE-PER nuclear and cytoplasmic extraction kit (Abcam). Briefly, 1×10^6 cells were harvested with trypsin-EDTA and then centrifuged at 500×g for 5 min. Next, the cell pellets were washed with PBS and centrifuged at 500×g for 5 min. To get the cytoplasmic extracts, the supernatant was removed and discarded, and 100 μl of ice-cold 1X pre-extraction buffer was added to the cell pellet. The tube was vortexed vigorously for 10 s, incubated on ice for 10 minutes, and centrifuged at 16,000×g for 2 min. The supernatant containing the cytoplasmic fraction was transferred to a new tube. To get the nuclear extract, the pellet fraction was suspended in 100 μl of ice-cold NER buffer, the tube was vortexed vigorously for 15 s, and the sample was placed on ice and vortexed for 5 s every 3 min during a period of 10 minutes. After a final centrifugation at 16,000×g for 5 min, the supernatant containing the nuclear fraction was transferred to a new tube. The cytoplasmic and nuclear extracts were collected and used for western blotting.

Immunoprecipitation and Western Blotting

Western blotting was carried out as described in reference[4]. In brief, cells were homogenized and lysed at 4°C in lysis buffer with protease and phosphatase inhibitors (Thermo Fisher #A32961). Cell lysates were sonicated and centrifuged at 12,000 ×g for 10 min at 4 °C, and the resulting supernatant was used for immunoblotting analysis. Protein concentrations in cell lysates were measured using Beyotime Protein Assay Dye Reagent. For co-immunoprecipitation, cells were transfected with the indicated expression plasmids for 24 to 48 hr. Whole cell lysates were prepared with NP40 buffer (Beyotime) supplemented with protease and phosphatase inhibitors. Cell lysates were sonicated, centrifuged, and pre-cleared with normal IgG and protein A/G beads for 3 hr to reduce non-specific binding. Then, pre-cleared cell lysates were incubated with their respective antibodies overnight and with protein A/G beads for another 3 hr at

4°C. The agarose beads were washed extensively and eluted by boiling at 100°C for 5 min. The precipitates were then analyzed by immunoblotting.

Glucose Uptake

Glucose uptake was measured using the Glucose Uptake-Glo™ Assay kit (Promega #tm467) according to according to the manufacturer's instructions. Briefly, cells were seeded 8000 per/well in 96-well plates. and cultured in normal medium overnight.

The medium was removed, and cells were washed with 100 µl PBS to most efficiently remove glucose from the cell culture. Cells were added to 50 µl of the prepared 1mM 2DG per well and incubated for 10 min at room temperature. After adding the 2DG6P detection reagent, luminescence was recorded using a 0.3–1 second integration on a luminometer (BioTek).

Acetyl CoA Activity Assay

Acetyl CoA activity assay was performed using Acetyl CoA fluorometric assay kit (BioVision, cat. k312-100) according to the manufacturer's instructions. Briefly, cells were collected and deproteinized using a perchloric acid/KOH (BioVision, cat. k808-200). Samples were added to 10 µl CoA quencher and quench remover to correct background. Finally, cells were added to a 50 µl reaction mix buffer to measure fluorescence using Ex/Em=535/587 nm.

Metabolic Profiling and Isotope Tracing

Isotope tracing experiments were performed as previously described[35]. Cells were cultured with medium containing [U-13C]-labeled glucose (sigma) for 24 h. For extraction of intracellular metabolites, cells were collected with 70% methanol extraction for LC-MS/MS. Cells (2×10^7) per sample (in triplicates) were harvested for metabolomics analysis performed by Metabolon Inc.

Xenograft Mouse Model

A549 cells (1×10^7 cells) were inoculated into the lower flanks of 4-week-old Balb/c nude mice (n=10 per group). Mice were euthanized when tumor size reached the limitation of 1500 mm3 and tumors were isolated and weighed after 35 days. To determine the effect of HMGA1 on tumor growth in vivo, A549 cells (2×10^6 cells) were inoculated subcutaneously into an additional 4-week-old Balb/c nude mice(n=14). 10 OD cholesterol - modified HMGA1siRNA and control siRNA was administered at the bottom of the tumor every 3 days when the tumor volume was about 500 mm3. One weeks after the injection, the mice were euthanized**,** and the tumors were removed. All animals were cared for according to the Association for the Assessment and Accreditation of Laboratory Animal Care. All animal procedures were approved by the Subcommittee on Research Animal Care at West China Hospital of Sichuan University.

Statistical Methods

The statistical methods are described in each figure. All analyses were performed using Graph Pad Prism 7. Data are given as means and standard errors. Groups which 2 groups, experimental vs control were compared with two-tailed, unpaired Student's t-tests. Asterisks in the figures indicate statistical significance (*p < 0.05; **p < 0.01; ***p < 0.001).

Data Availability

All data supporting the findings of this study are available in the article and its supplementary material or from the corresponding authors on reasonable request.

Declarations

Author Contributions

L.Z. and Y.H.Z. contributed to writing the manuscript; Y.Y. performed immunohistochemistry and immunofluorescence staining; B.H contributed to design and edit article; H.H. and J.J.R. contributed to the acquisition and analysis of data; L.W.Q. and M.F.L. contributed to the animal experiments and determined cell proliferation; M.L.Y. and T.T.S measured metabolites; Y.Y.F,Y.Y.N. T.T.G, N.N.C. and Z.Q.L. reviewed the manuscript for critical content; W.M.L. contributed to the experiment design.

Competing Interests: The authors declare no competing interests.

Acknowledgements

This work was supported by grants from National Natural Science Foundation of China (81974363 and 81772478); Sichuan International / Hong Kong, Macao and Taiwan Science and technology innovation cooperation project: molecular imaging research on targeted treatment of lung cancer (2018hh0161).

References

1. Boucher, J. et al. Apelin, a newly identified adipokine up-regulated by insulin and obesity. *Endocrinology*. **146**, 1764-1771 (2005).
2. Chapman, N. A., Dupre, D. J. & Rainey, J. K. The apelin receptor: physiology, pathology, cell signalling, and ligand modulation of a peptide-activated class A GPCR. *Biochem. Cell Biol.* **92**, 431-440 (2014).
3. Berta, J. et al. Apelin expression in human non-small cell lung cancer: role in angiogenesis and prognosis. *J. Thorac. Oncol.* **5**, 1120-1129 (2010).
4. Harford-Wright, E. et al. Pharmacological targeting of apelin impairs glioblastoma growth. *Brain*. **140**, 2939-2954 (2017).
5. Hoffmann, M., Fiedor, E. & Ptak, A. Bisphenol A and its derivatives tetrabromobisphenol A and tetrachlorobisphenol A induce apelin expression and secretion in ovarian cancer cells through a peroxisome proliferator-activated receptor gamma-dependent mechanism. *Toxicol. Lett.* **269**, 15-22 (2017).

6. Picault, F. X. et al. Tumour co-expression of apelin and its receptor is the basis of an autocrine loop involved in the growth of colon adenocarcinomas. *Eur. J. Cancer*. **50**, 663-674 (2014).
7. Lin, Z. Y. & Chuang, W. L. Hepatocellular carcinoma cells cause different responses in expressions of cancer-promoting genes in different cancer-associated fibroblasts. *Kaohsiung J. Med. Sci.* **29**, 312-318 (2013).
8. Chen, T. et al. Apelin13/APJ promotes proliferation of colon carcinoma by activating Notch3 signaling pathway. *Oncotarget*. **8**, 101697-101706 (2017).
9. Peng, X. et al. Apelin-13 induces MCF-7 cell proliferation and invasion via phosphorylation of ERK1/2. *Int. J. Mol. Med.* **36**, 733-738 (2015).
10. Feng, M., Yao, G., Yu, H., Qing, Y. & Wang, K. Tumor apelin, not serum apelin, is associated with the clinical features and prognosis of gastric cancer. *Bmc Cancer*. **16**, 794 (2016).
11. Podgorska, M., Pietraszek-Gremplewicz, K. & Nowak, D. Apelin Effects Migration and Invasion Abilities of Colon Cancer Cells. *Cells*. **7**, (2018).
12. Uribesalgo, I. et al. Apelin inhibition prevents resistance and metastasis associated with anti-angiogenic therapy. *Embo Mol. Med.* **11**, e9266 (2019).
13. Ackerman, D. & Simon, M. C. Hypoxia, lipids, and cancer: surviving the harsh tumor microenvironment. *Trends Cell Biol.* **24**, 472-478 (2014).
14. Chen, M. & Huang, J. The expanded role of fatty acid metabolism in cancer: new aspects and targets. *Precis Clin Med*. **2**, 183-191 (2019).
15. Cheng, C. et al. Glucose-Mediated N-glycosylation of SCAP Is Essential for SREBP-1 Activation and Tumor Growth. *Cancer Cell*. **28**, 569-581 (2015).
16. Rysman, E. et al. De novo lipogenesis protects cancer cells from free radicals and chemotherapeutics by promoting membrane lipid saturation. *Cancer Res.* **70**, 8117-8126 (2010).
17. Wakil, S. J. & Abu-Elheiga, L. A. Fatty acid metabolism: target for metabolic syndrome. *J. Lipid Res.* **50 Suppl**, S138-S143 (2009).
18. Currie, E., Schulze, A., Zechner, R., Walther, T. C. & Farese, R. J. Cellular fatty acid metabolism and cancer. *Cell Metab.* **18**, 153-161 (2013).
19. Horton, J. D., Goldstein, J. L. & Brown, M. S. SREBPs: activators of the complete program of cholesterol and fatty acid synthesis in the liver. *J. Clin. Invest.* **109**, 1125-1131 (2002).
20. Karin, M. New insights into the pathogenesis and treatment of non-viral hepatocellular carcinoma: a balancing act between immunosuppression and immunosurveillance. *Precis Clin Med*. **1**, 21-28 (2018).
21. Dray, C. et al. Apelin stimulates glucose utilization in normal and obese insulin-resistant mice. *Cell Metab.* **8**, 437-445 (2008).
22. Huang, J., Kang, S., Park, S. J. & Im, D. S. Apelin protects against liver X receptor-mediated steatosis through AMPK and PPARalpha in human and mouse hepatocytes. *Cell. Signal.* **39**, 84-94 (2017).

23. Massiere, F. & Badet-Denisot, M. A. The mechanism of glutamine-dependent amidotransferases. *Cell. Mol. Life Sci.* **54**, 205-222 (1998).
24. Cluntun, A. A., Lukey, M. J., Cerione, R. A. & Locasale, J. W. Glutamine Metabolism in Cancer: Understanding the Heterogeneity. *Trends Cancer*. **3**, 169-180 (2017).
25. Zhao, J. et al. Deamidation Shunts RelA from Mediating Inflammation to Aerobic Glycolysis. *Cell Metab.* **31**, 937-955 (2020).
26. Guillet-Deniau, I. et al. Glucose induces de novo lipogenesis in rat muscle satellite cells through a sterol-regulatory-element-binding-protein-1c-dependent pathway. *J. Cell Sci.* **117**, 1937-1944 (2004).
27. Ha, T. K. et al. Caveolin-1 increases aerobic glycolysis in colorectal cancers by stimulating HMGA1-mediated GLUT3 transcription. *Cancer Res.* **72**, 4097-4109 (2012).
28. Xu, S. et al. In vivo, ex vivo, and in vitro studies on apelin's effect on myocardial glucose uptake. *Peptides*. **37**, 320-326 (2012).
29. Attane, C. et al. Apelin treatment increases complete Fatty Acid oxidation, mitochondrial oxidative capacity, and biogenesis in muscle of insulin-resistant mice. *Diabetes*. **61**, 310-320 (2012).
30. Li, Y. et al. Apelin-13 Is an Early Promoter of Cytoskeleton and Tight Junction in Diabetic Macular Edema via PI-3K/Akt and MAPK/Erk Signaling Pathways. *Biomed Res. Int.* **2018**, 3242574 (2018).
31. Falvo, J. V., Thanos, D. & Maniatis, T. Reversal of intrinsic DNA bends in the IFN beta gene enhancer by transcription factors and the architectural protein HMG I(Y). *Cell*. **83**, 1101-1111 (1995).
32. Shah, S. N. & Resar, L. M. High mobility group A1 and cancer: potential biomarker and therapeutic target. *Histol. Histopathol.* **27**, 567-579 (2012).
33. Han, Y. et al. Post-translational regulation of lipogenesis via AMPK-dependent phosphorylation of insulin-induced gene. *Nat. Commun.* **10**, 623 (2019).
34. Matsuda, M. et al. SREBP cleavage-activating protein (SCAP) is required for increased lipid synthesis in liver induced by cholesterol deprivation and insulin elevation. *Genes Dev*. **15**, 1206-1216 (2001).
35. Brown, A. J., Sun, L., Feramisco, J. D., Brown, M. S. & Goldstein, J. L. Cholesterol addition to ER membranes alters conformation of SCAP, the SREBP escort protein that regulates cholesterol metabolism. *Mol. Cell*. **10**, 237-245 (2002).
36. Coloff, J. L. et al. Differential Glutamate Metabolism in Proliferating and Quiescent Mammary Epithelial Cells. *Cell Metab.* **23**, 867-880 (2016).

Figures

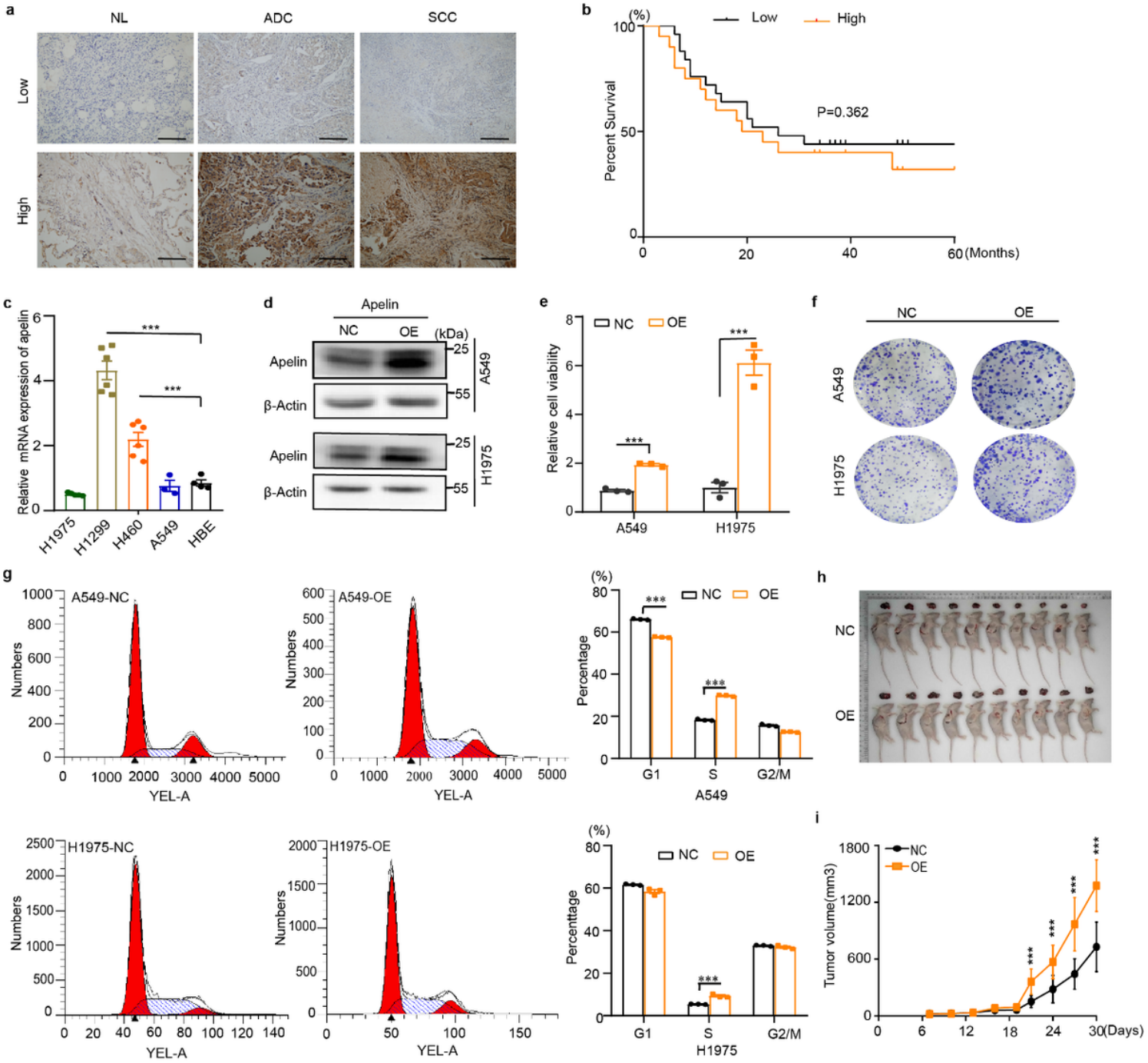

Figure 1

Apelin promoted the proliferation of lung cancer cells. a. Immunohistochemical staining for apelin expression in lung tumor tissues and distal normal tissues. Staining intensity was classified as low and high groups. NL, normal lung tissue; ADC, adenocarcinoma tissue; SCC, squamous carcinoma tissue. Scale bar□50 μm. b. Kaplan-Meier curves for the overall survival of the patient with non-small-cell lung cancer (NSCLC), according to apelin expression as determined by immunohistochemistry, n = 51. c. Apelin mRNA expression in both tumor (A549, H1299, H446, H1975 and H460) and normal (HBE) cell lines. d. Apelin in A549-OE and H1975-OE cells. β-Actin was used as an internal control. NC, negative control; OE, over-expression. e. Viability of apelin-overexpressed cells (A549-OE and H1975-OE) and

negative controls as measured by Cell Counting Kit-8. f. Colony formation in apelin-overexpressed cells (A549-OE and H1975-OE) and negative controls. g. Cell-cycle detection by flow cytometry in apelin-overexpressed cells (A549-OE and H1975-OE) and negative controls. h. Subcutaneous tumors in A549-OE and A549-NC in nude mice (n=10 per group). i. Tumor volumes in A549-OE and A549-NC in nude mice. Data are presented as the mean ± SEM, unpaired two-tailed Student's t-test. * P<0.05 ** P<0.01 *** P<0.001.

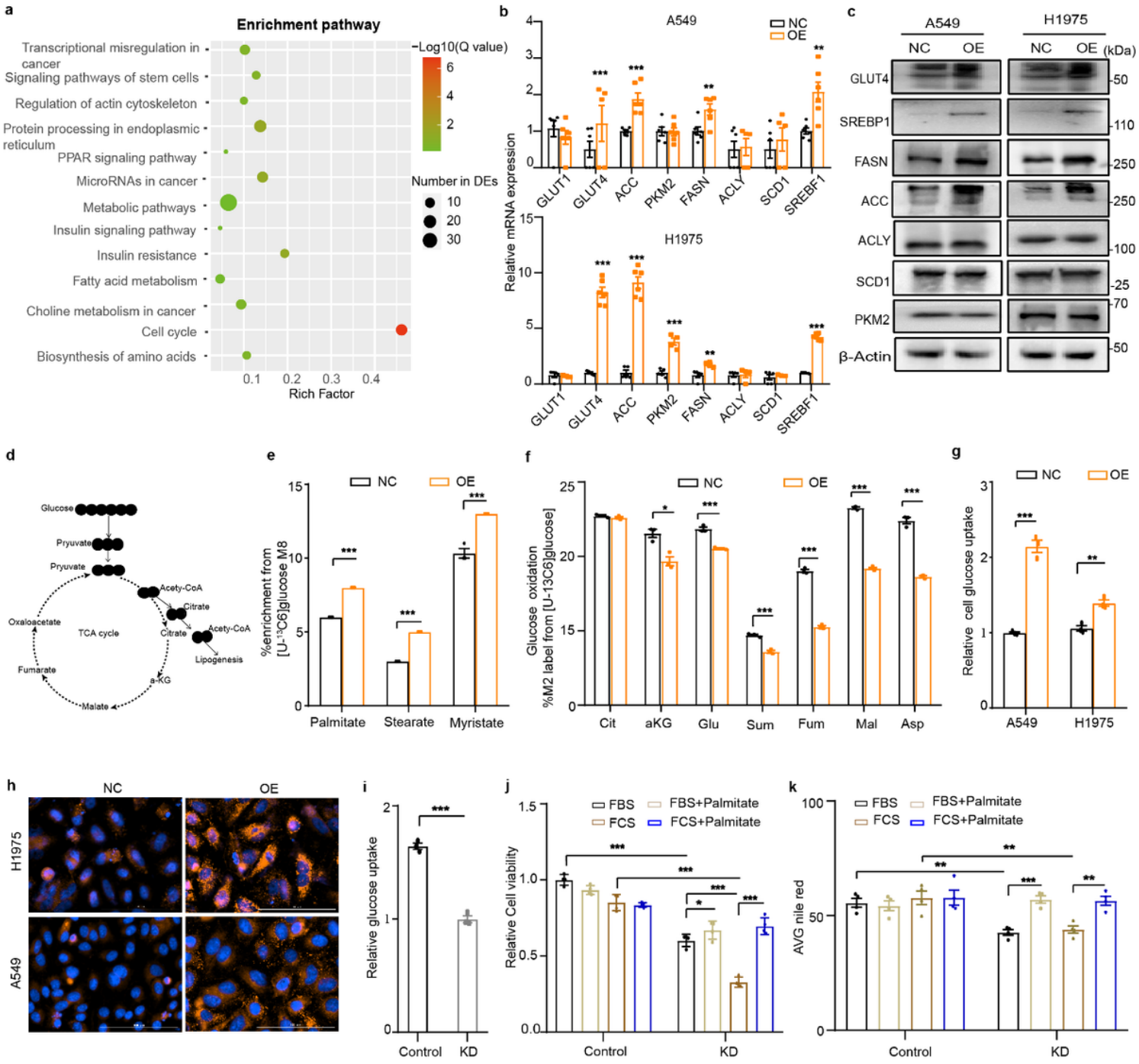

Figure 2

Apelin promoted lung cancer cells growth by enhancing de novo fatty acid synthesis a. Signalling enrichment pathway in A549-OE and –NC cells by RNA-Seq analysis. b. Expression of lipid-synthesis-related genes in both A549-OE (top) and H1975-OE (bottom) cells. c. Lipid-synthesis-related genes in A549-OE (left) and H1975-OE (right) cells. d. The carbon atom (circles) transitions and tracers used to detect de novo fatty acid synthesis. The isotopic label from [U-13C6] glucose (black circles) changed into pryuvate and was converted to citrate in mitochondrial export and transfer to Acetyl-CoA and synthetic fatty acid in cytoplasm, rather than enter into the tricarboxylic acid cycle. e. Saturated fatty acid enrichment labeling from [U-13C6] glucose cells in A549-OE and –NC cells. f. Glucose oxidation from a 13C metabolic flux analysis model in A549-OE and –NC cells cultured with [U-13C6] glucose. g. Glucose uptake in A549-OE and H1975-OE cells. h. Lipid contents in A549-OE and H1975-OE cells. Nile red stain. Scale bar = 100 μm. i. Glucose uptake in H460-control, and –KD cells. j. Cell viability in H460-control, and –KD cells in medium containing FBS ± 200 μM exogenous palmitate (PA) for 72 h. k. Measurements of cellular fatty acid content in H460-control, and –KD cells treated with FBS and FCS ± 200 μM exogenous palmitate (PA) for 72 h. For all measurements, values (n=3-6) were recorded. Data are from one of least two separate experiments. Data are presented as the mean ± SEM, unpaired two-tailed Student’s t-test. * $P<0.05$ ** $P<0.01$ *** $P<0.001$.

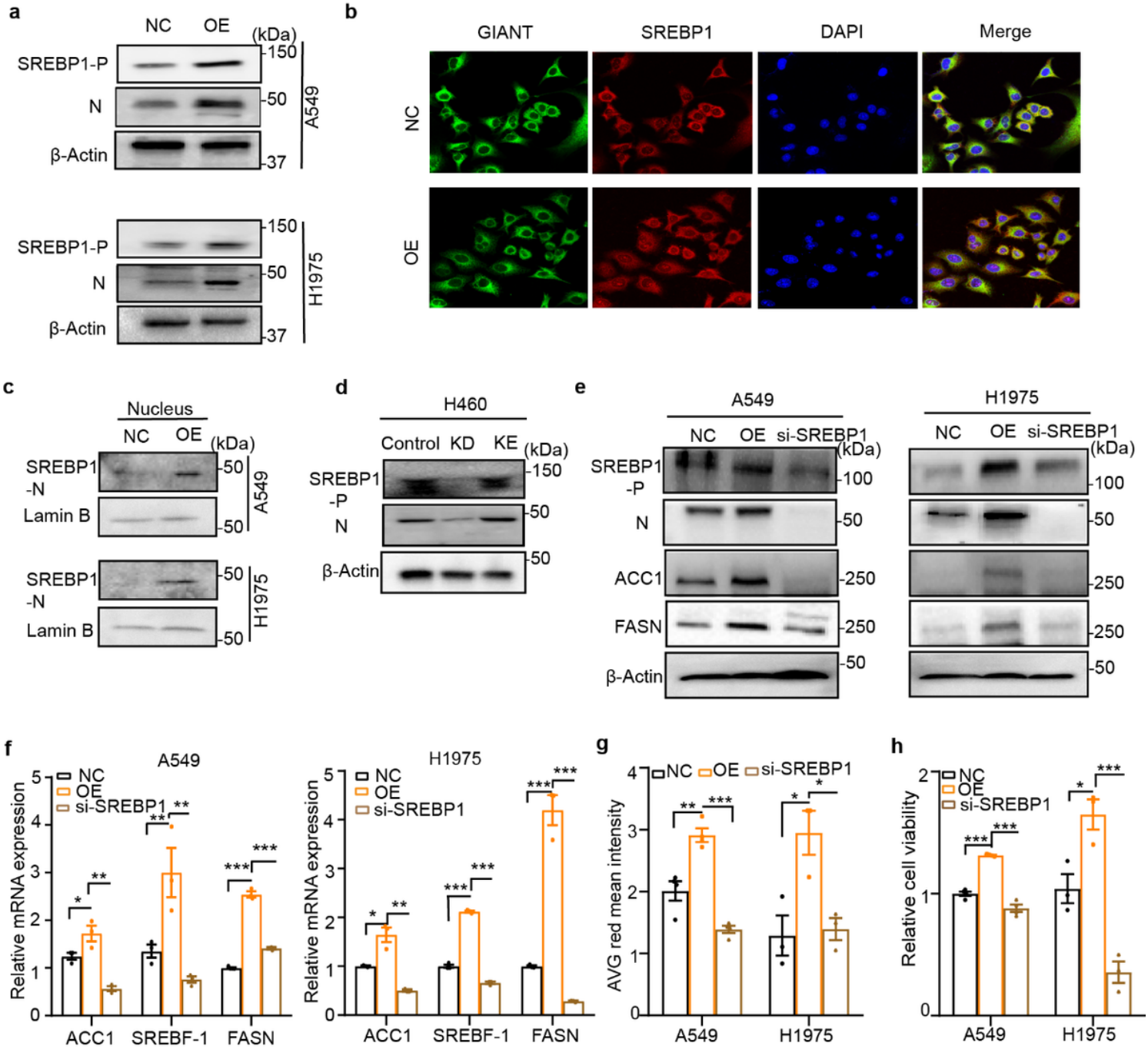

Figure 3

Apelin promoted the release of SREBP-1 cleavage and increased expression of lipid-related proteins. a. Mature proteins (SREBP1-N) and precursor-SREBP1 (SREBP1-P) in A549-OE and H1975-OE cells. β-Actin was used as an internal control. b. Confocal microscopy images indicated SREBP1 trafficking related to the Golgi apparatus in A549-OE cell. DAPI: nucleus staining; Giant: Marker for Golgi apparatus. Scale bar: 20 μm. c. The nuclear translocation of SREBP1-N detection in A549 and H1975-OE cells. d. Mature proteins (SREBP1-N) and precursor-SREBP1 (SREBP1-P) in H460 control, -KD and -KE cells. β-Actin was used as an internal control. e. Mature proteins (SREBP1-N) and precursor-SREBP1 (SREBP1-P), as well as lipid-related proteins treated by siRNA-SREBP1 in A549-OE and H1975-OE cells. f. Relative expression of important enzymes in A549-OE and H1975-OE cells treated by siRNA-SREBP1. g. Cellular lipid contents in

H1975-OE and A540-OE cells treated with siRNA-SREBP1. h. Cell viability in H1975-OE and A540-OE cells treated with siRNA-SREBP1. For all measurements, values (n=3-6) were recorded. Data are from one of least two separate experiments. Data are presented as the mean ± SEM, unpaired two-tailed Student's t-test. * P<0.05 ** P<0.01 *** P<0.001.

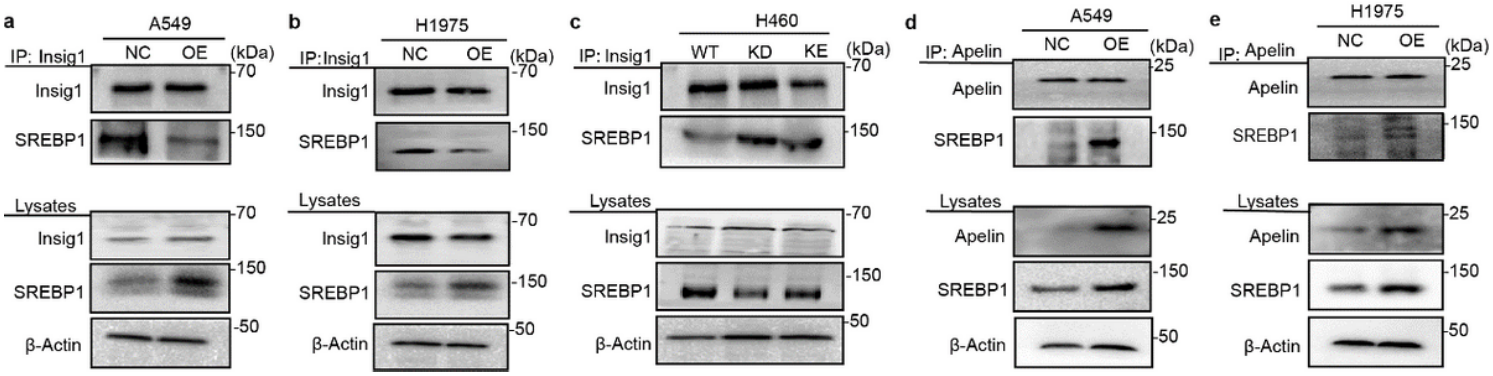

Figure 4

Apelin interacts with SREBP1 by inhibiting SREBP1 from binding to Insig1 a, b. Immunoprecipitation detected SREBP1 disassociation with Insig-1 in A549-OE and H1975-OE cells. c. Immunoprecipitation detected increased interaction between SREBP1 and INSIG1 in knock-down of apelin H460 cells. d. Immunoprecipitation detected binding of SREBP1 to apelin in A549-OE and H1975-OE cells.

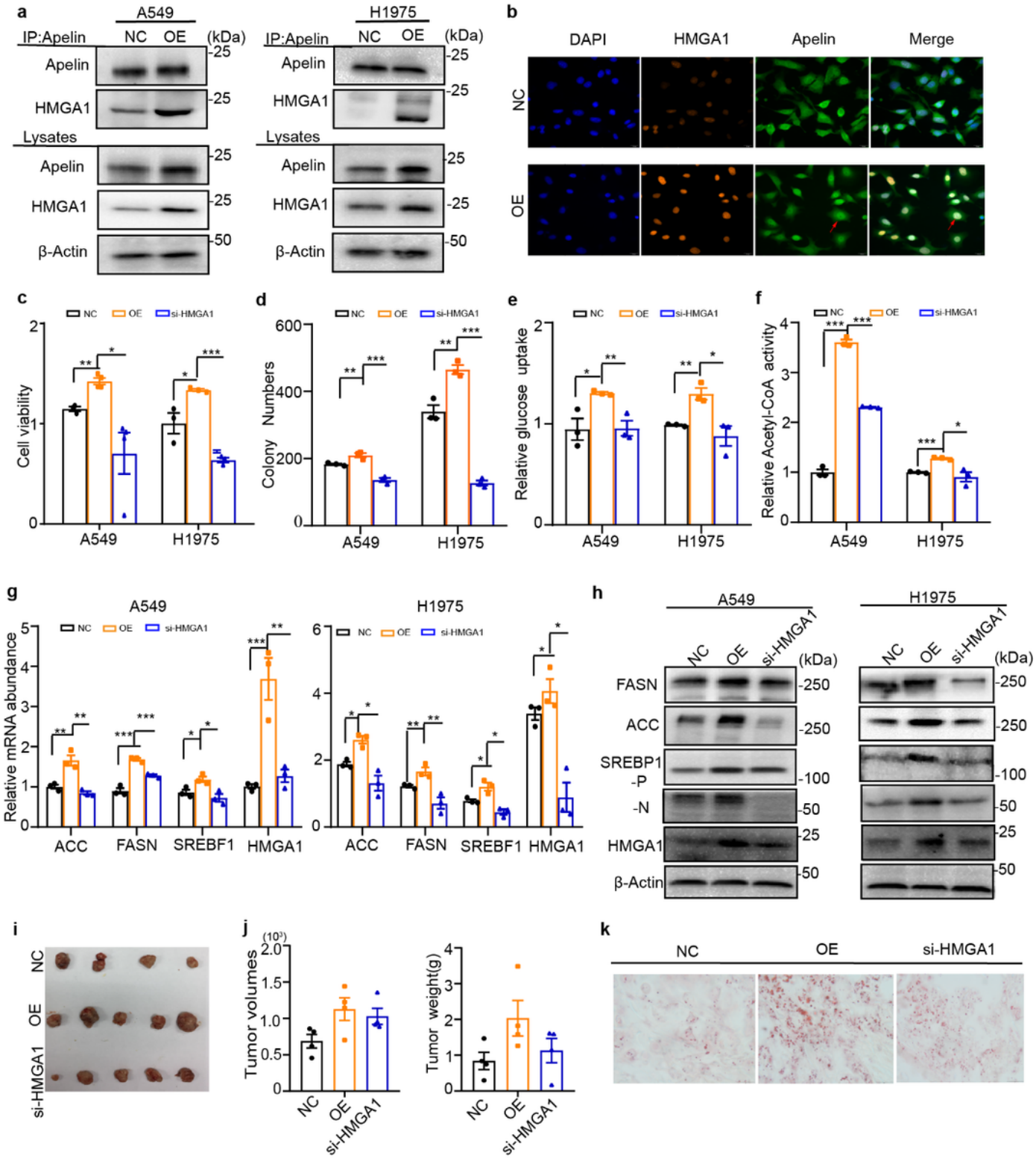

Figure 5

Apelin-HMGA complexes activated SREBP1 and increased expression of lipid synthesis related genes. a. Immunoprecipitation detected apelin-HMGA1 interaction in A549-OE (left) and H1975-OE (right) cells. β-Actin was used as internal control. b. Immunofluorescence detected the nuclear localization of apelin and HMGA1 in A549 NC and -OE cells. Scale bar: 25μm. c. Cell viability in H1975-OE and A540-OE cells treated with siRNA-HMGA1. d. Colony formation in H1975-OE and A540-OE cells treated with siRNA-HMGA1. e.

Glucose uptake in H1975-OE and A540-OE cells treated with siRNA-HMGA1. f. Relative Acetyl-CoA activity in A549 -OE and H1975-OE cells treated with siRNA-HMGA1. g. Quantitative PCR detected the expression of lipogenic enzymes in A549-OE and H1975-OE cells treated with siRNA-HMGA1. h. Activity of SREBP1 (SREBP1-N), precursor SRBEP1 (SREBP1-P) and lipid-related protein in A549-OE and H1975-OE cells treated with siRNA-HMGA1. β-Actin was used as internal control. i. Subcutaneous tumor formation in nude mice implanted with A549-NC (n=4) and -OE (n=5) and –OE- siRNA-HMGA1 (n=5) groups. j. Tumor volumes and weights for negative controls (black, n-4), -OE (orange, n=5) and –OE with siRNA-HMGA1 (blue, n=5) groups. k. Oil red O staining for lipids in SCID mice implanted with (left to right) A549-NC (n=4), -OE (n=5) and –OE-siRNA-HMGA1 (n=5). For all measurements, values (n=3-4) were recorded. Data are from one of least two separate experiments. Data are presented as the mean ± SEM, unpaired two-tailed Student's t-test. * P<0.05 ** P<0.01 *** P<0.001.

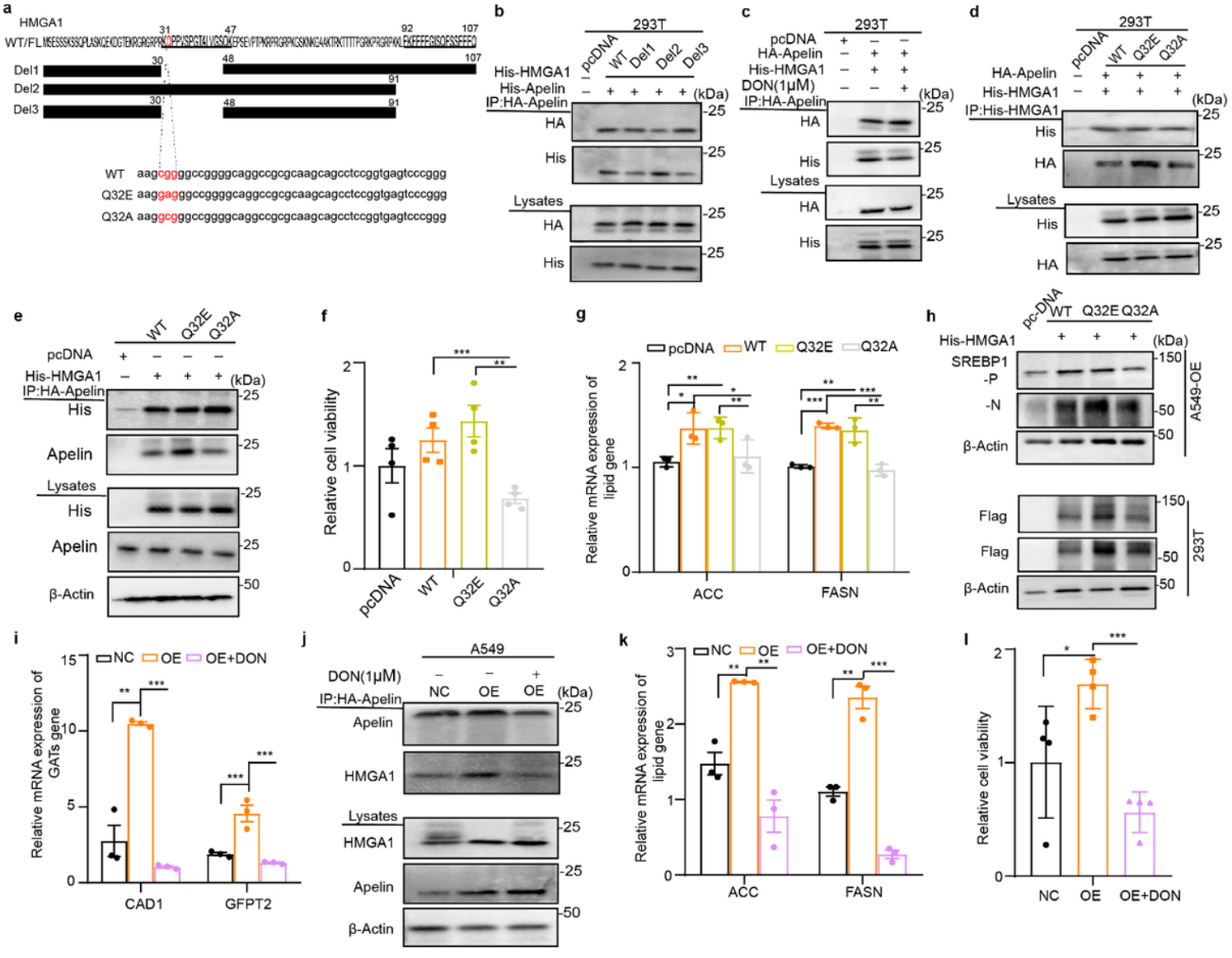

Figure 6

Deamidated HMGA1 elevated binding of apelin to HMGA1 and increased activity of SREBP1 a. Amino acid sequences of HMGA1 and binding sequences with apelin at 30-47 and 92-107 [bold font], relative to

deletion mutations Del1, Del2, and Del3. The genomic location of the deamidation sequence of HMGA1 Glu32, two HMGA1 mutants Q32E (glutamic acid, Glu), and Q32A (alanine, Ala) are showed in red. b. Immunoprecipitation results for proteins from HEK 293T cells co-expressing His-apelin with His-WT and truncated mutants of HMGA1 and analyzed for coprecipitated His after immunoblotting with the indicated antibodies. c. Immunoprecipitation results for proteins from HEK 293T cells co-expressing His-HMGA1 and HA-apelin in the presence or absence of DON (1 μM) for 24 hours and analyzed for coprecipitated proteins using the indicated antibodies. d. Immunoprecipitation results for HEK 293T cells expressing HA- apelin, His-WT- HMGA1 and deamidation mutants for HMGA1 Q32E and Q32A. e. Immunoprecipitation results for A549-OE cells expressing HA- apelin, His -WT- HMGA1 and deamidation mutants for HMGA1 Q32E and Q32A. f. Cell viability for A549-OE cells transfected with His-WT HMGA1 and His-HMGA1 deamidation mutants for HMGA1 mutants Q32E and Q32A. g. mRNA expression of SREBP-1, FASN, and ACC1 in A549-OE cells transfected with His-WT HMGA1 and His-HMGA1 deamidation mutants for HMGA1 mutants Q32E and Q32A. h. SREBP-1 cleavage in A549-OE expression HMGA1 and His-HMGA1 deamidation mutants and in 293T cells co-transfection with GFP-SREBP1 and His-HMGA1 deamidation mutants. i. Expression of glutamine amidotransferases (GATs) in A549-OE and -NC cells. j. Immunoprecipitation results for apelin binding with HMGA1 in A549-OE cells in the presence or absence of DON (1μM) for 24 hr. k. Quantitative PCR for expression of lipogenic genes in A549-OE and -NC cells in the presence or absence of DON (1μM) for 24 hr. l. Cell viability detection in A549-NC and –OE cells in the presence or absence of DON (1 μM) for 48 hr. For all measurements, values (n=3-5) were recorded. Data are from one of least two separate experiments. Data are presented as the mean ± SEM, unpaired two-tailed Student’s t-test. * $P<0.05$ ** $P<0.01$ *** $P<0.001$.

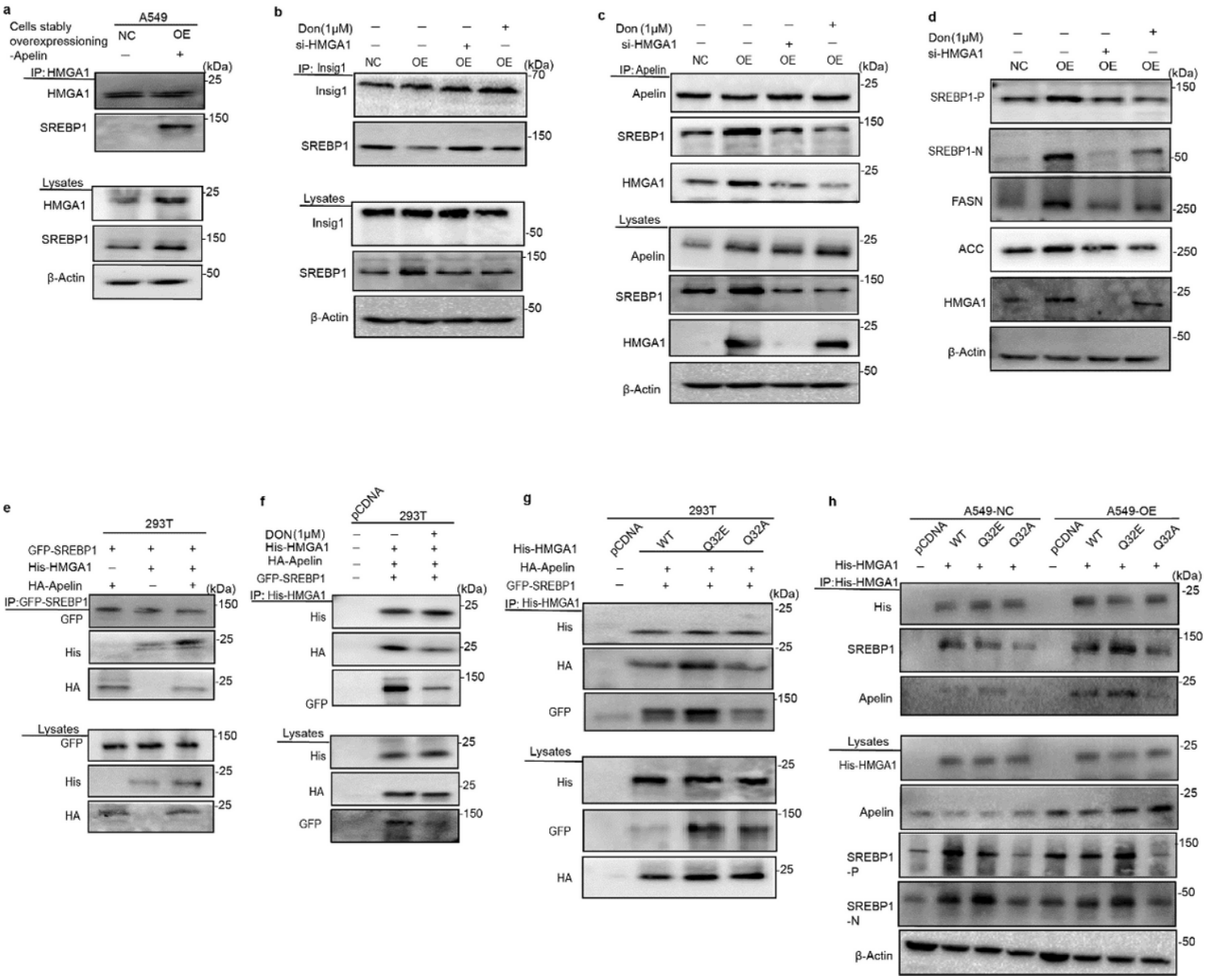

Figure 7

Deamidated HMGA1 promoted the formation of apelin-SREBP1- HMGA1 complexes a. Immunoprecipitation results for the binding of SREBP1 and HMGA1 in A549-OE cells. b, c. Immunoprecipitation results for A549-NC and –OE cells transfected with si-HMGA1 or addition of DON (1μM) for 24 hr. d. Western blot results of the activity of SREBP-1 and lipid-related proteins in A549-OE cells transfected with si-HMGA1 or after adding DON (1μM) for 24 hr. e. Immunoprecipitation results for HEK 293T cells expressing GFP-SREBP1 and HA- apelin with His -WT-HMGA1 for 24 hr. f. Immunoprecipitation results for HEK 293T cells expressing GFP-SREBP1 and HA- apelin with His -WT-HMGA1 in the presence or absence of DON (1μM) for 24 hr. g. Immunoprecipitation results for proteins in HEK 293T cells co-expressing GFP-SREBP1 and HA-apelin with His-WT or His-HMGA1deamidation mutants for 24 hr. h. Immunoprecipitation results for A549-NC and–OE cells expressing His- WT HMGA1 or His-HMGA1 deamidation mutants for HMGA1 mutants Q32E and Q32A for 48 hr.

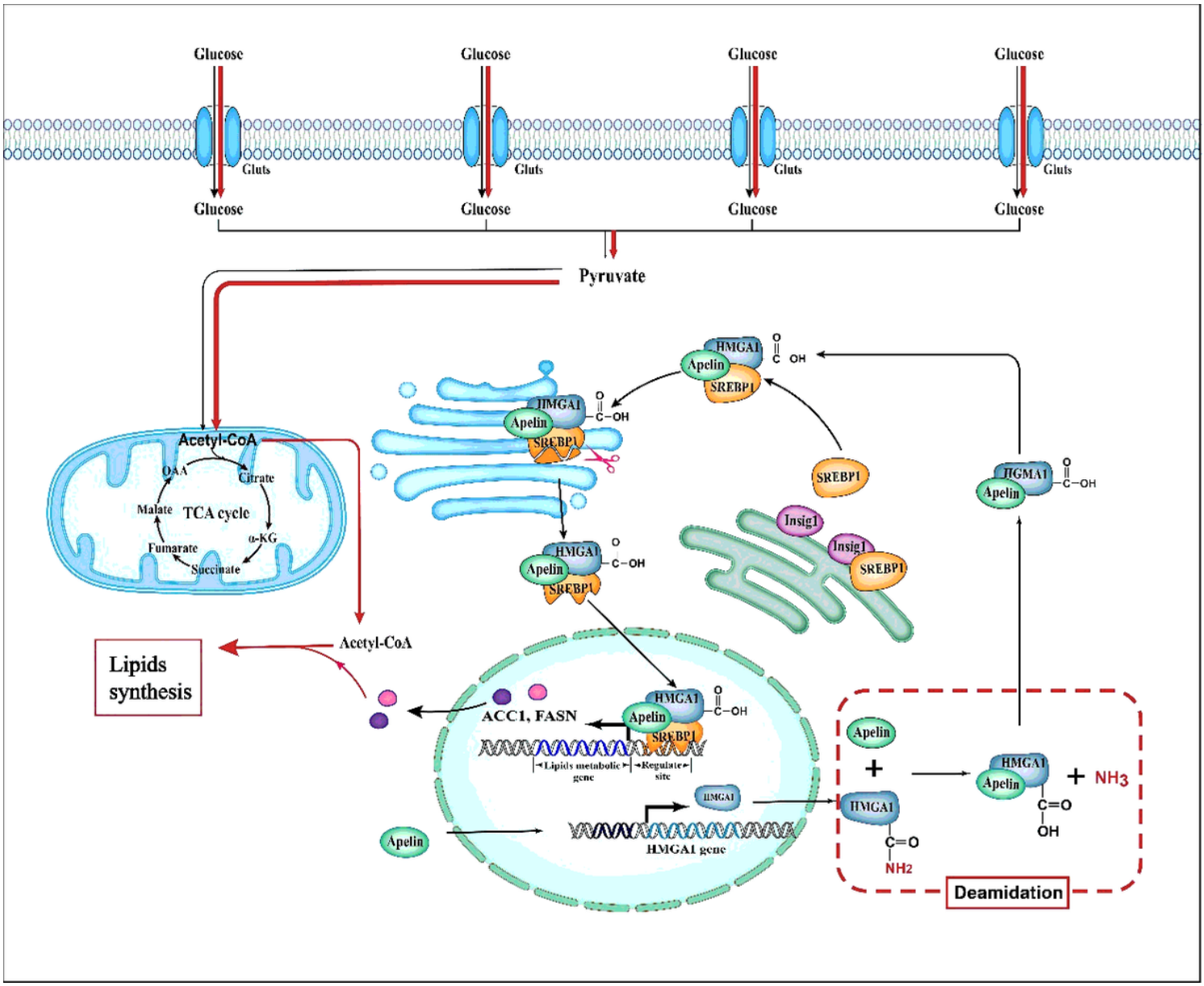

Figure 8

Proposed Mechanism of Apelin promotes tumorigenesis by enhancing SRBEP1 activity and Lipid Synthesis In brief, apelin increases of lipogenesis to promote cell proliferation. With the overexpression of apelin, lung cancer cells increase glucose uptake (red bold lines) and change the cellular carbohydrate metabolism pathway from TCA cycle to fatty acid de novo synthesis. SREBP1 is an important regulator of fatty acid synthesis. Dissociated from Insig1, hydrolysis of activated SREBP1 releases active transcription fragments that regulate lipid genes ACC1 and FASN. As a transcription enhancer, HMGA1 interacts with transcription factors to regulate gene expression. Apelin binds to HMGA1 for deamidation of HMGA1(red dashed frame). Deamidation of HMGA1 increases the affinity of protein interactions. Apelin deamidate HMGA1 for enhancing the formation of the Apelin-HMGA1-SREBP1 complexes. Deamidated HMGA1 increases the activity of SREBP1 and its dissociation from Insig1. Thus, the apelin/HMGA1/SREBP complexes can traffic to the Golgi, resulting in SREBP cleavage and its nuclear function. In this model, the deamidation of HMGA1 mediated apelin/HMGA1/SREBP1 trafficking and the

subsequent SREBP activation to promote tumor growth. ER, Endoplasmic reticulum; SREBP1, Sterol regulatory-element-binding protein 1; Insig1, insulin-induced gene protein 1; TCA cycle, tricarboxylic acid cycle.

Supplementary Files

This is a list of supplementary files associated with this preprint. Click to download.

- SupplementaryTables.pdf
- Fs1.png
- Fs2.png
- Fs3.png
- Fs4.png
- Fs5.png